Geofísica Internacional (2000), Vol. 39, Num. 2, pp. 179-188

Nonlinear 3-D inversion of gravity data over a sulfide ore body

J. García-Abdeslem[1]

[1] *CICESE, División de Ciencias de la Tierra, Departamento de Geofísica Aplicada, Ensenada, B. C., México.*

Received: February 19, 1999; accepted: January 14, 2000.

RESUMEN

El gradiente gravimétrico horizontal y el principio de superposición de campos potenciales son utilizados en la interpretación de los datos gravimétricos de un yacimiento de sulfuros mediante una estructura 3-D de densidades. El yacimiento está constituido por sulfuros masivos y diseminados, principalmente de esfalerita, alojados en caliza. El gradiente horizontal de la anomalía gravimétrica permitió inferir en forma aproximada la extensión lateral del yacimiento. La interpretación de los datos gravimétricos se propone como un problema inverso que se realiza en forma iterativa, siguiendo un criterio de mínimos cuadrados con amortiguamiento. El modelado inverso está acotado con valores de densidades y espesor del yacimiento, obtenidos a partir de un pozo perforado sobre la zona mineralizada.

PALABRAS CLAVE: México, Zacatecas, yacimientos minerales, gravimetría, gradiente horizontal, inversión no-lineal 3-D.

ABSTRACT

The horizontal gravity gradient and the principle of superposition of potential fields are used in the interpretation of gravity data from a sulfide ore body in terms of a 3-D structure of densities. The ore body is constituted of massive and disseminated sulfides, mainly of sphalerite, hosted in limestone. The horizontal gradient of the gravity anomaly lead to a rough estimate of the lateral extent of the ore body. The interpretation of the gravity data is posed as an inverse problem, and carried out iteratively, following a damped least-squares criteria. The inverse modeling was constrained with information on densities and thickness of the ore body, obtained from a borehole drilled over the ore body.

KEY WORDS: México, Zacatecas, mineral deposits, gravimetry, horizontal gradient, 3-D non-linear inversion.

INTRODUCTION

In the interpretation of residual Bouguer gravity anomalies, one attempts to find both the geometry and the density of a geological reasonable source body, such that its gravity effect explains the observed gravity. However, to constrain our models we must include other independent information, generally related with the geometry and density of the source body, in order to reduce the large number of underground density distributions compatible with the gravity data.

Residual Bouguer gravity anomalies, in general, consist of positive and negative values. These are interpreted as being caused by lateral changes in the density contrast of the rocks, with respect to the Bouguer density. A common practice followed by most interpreters when selecting a model for interpretation, is to examine the aspect ratio (length/width) of the gravity anomaly. The use of two-dimensional models seems to be appropriate when the minimum aspect ratio is greater than five (García-Abdeslem, 1996). 2-D models are useful in addressing geologic problems where density varies in the transect direction and along the vertical direction. Besides the aspect ratio of the gravity anomaly, in a 2-D model the topography must also be reasonably invariant along the direction normal to the transect. When the aspect ratio is less than five and topography varies in a direction normal to the transect, a 3-D model is required for the appropriate interpretation of the data.

Several authors have addressed the 3-D modeling and inversion of gravity data in both the spatial domain and in the wavenumber domain. Cordell and Henderson (1968) carried out one of the first attempts of 3-D nonlinear modeling in the spatial domain. They used the Bouguer slab formula on gridded data as a first approach to the structure, which thus is further refined by a bundle of prisms, following an iterative least-squares method. Chai and Hinze (1988) have proposed a method for modeling the gravity effect caused by a collection of vertical prisms, where density varies with depth following an exponential function. The performance of this method is dependent of the use of a shift-sampling technique for computing the inverse Fourier transform. García-Abdeslem (1992) developed a spatial domain method suitable for 2- and 3-D forward modeling and inversion of the gravity effect caused by a vertical prism, where density varies with depth according to any well behaved function. Zeyen and Pous (1993) proposed a method to simultaneously

invert gravity and magnetic data to derive a 3-D model; the joint inversion of gravity and magnetic data, and the use of *a priori* information helps to reduce the ambiguity in the interpretation. Bear *et al*. (1995) developed a method for linear inversion of gravity data for 3-D density distributions that uses a Levenberg-Marquardt damping parameter to control the convergence of the method. Madeiros and Silva (1995) developed a 3-D gravity interpretation method based on the inversion of source moments to characterize the position and orientation of the source body. Recently, García-Abdeslem (1995) developed a 3-D wavenumber domain method for forward modeling and nonlinear inversion of gravity data to obtain both density and geometry of the source body.

In this work, gravity data collected over a sulfide ore body located in Zacatecas, Mexico, are interpreted following a 3-D nonlinear inversion procedure that uses the principle of superposition of potential fields. The model, which consist of a collection of prisms of constant mass density, is constrained with additional independent information from a borehole. The lateral extent of the ore body is inferred from a gravity gradient analysis.

GEOLOGY

The study area is located in the eastern flank of the southern Sierra Madre Occidental, near the northwestern limit of the Mesa Central physiographic province (Salas, 1975). For much of its length, the Sierra Madre Occidental is a 2000 m above sea level (asl) plateau made up by flat-lying mid-Cenozoic rhyolitic ignimbrites. The southern part of the Zacatecas State (Figure 1) is characterized by a series of grabens that indicate an east-west directed episode of extension, that Henry and Aranda-Gómez (1992) have interpreted to be the southernmost expression of the Neogene Basin and Range extensional province of North America.

A generalized stratigraphic column of the study area is shown in Figure 2. The base of the column is formed by metasedimentary rocks of the Late Triassic Pimienta Fm., that is exposed east of Zacatecas City (Ponce and Clark, 1982). The Pimienta Fm. is intruded by the so-called "Rocas Verdes de Zacatecas" (greenstones). Burckhardt and Scalia (1906, in Ponce and Clark, 1982) recognized two penecontemporaneous groups of greenstones. The first group, that spans the time from Late Jurassic to Early Cretaceous, is known as the Chilitos Fm. and is formed by spilitic lavas, representing submarine eruptions consisting of pillow lavas of basaltic composition and andesite lava flows (CRM, 1991). The second group is a microdiorite that crops out north of Zacatecas City (Ponce and Clark, 1982).

Overlying the greenstones there is a transgresive sequence (Figure 2) comprised of a siltstone-sandstone unit, a shale-limestone unit, and a limestone-shale unit. This sequence, thought to be of early Cretaceous age, shows a lateral facies change to argillite. This change in the depositional environment is interpreted to be the result of a global sea level rise during Early Cretaceous time (Vail *et al*., 1977). The limestone at the top of the Early Cretaceous sedimentary sequence hosts the sulfide ore body.

Resting unconformably over the Cretaceous limestone (Figure 2) is the Paleocene-Eocene age Conglomerado Rojo Zacatecas (CRM, 1991). This polymictic conglomerate is exposed southeast of Zacatecas City but it is absent in the study area. It is composed of gravel fragments and red sandstones with some horizons of silt and clay and volcaniclastic and epiclastic materials (Ponce and Clarke, 1982). The youngest rocks are represented by intrusives affecting the Mesozoic sedimentary sequence, and associated volcanic rocks and dikes of rhyolitic composition.

A simplified geologic map of the study area is shown in Figure 3. The topsoil and Quaternary alluvium that covers most of the study area, is about 1-2 m thick within the central part of the polygon of the gravity survey. From water-supply drillholes, this unit is known to be thicker (> 200 m) towards the east and south, being apparently controlled by regional normal faults (Figure 3). The transgressive sequence, consisting of shale with limestone horizons and limestone with shale horizons, crops out west of the study area, and changes laterally to the limestone unit that is exposed in the northern part of the study area. This last unit hosts the ore body.

GRAVITY STUDY

A total of 992 gravity stations were occupied along 16 NE-oriented transects, each transect separated by 200 m, with stations every 50 m, covering an area of about 11 km^2. A high quality topographic survey of the gravity stations position, and a strict control of instrumental drift allowed a high quality data set to be obtained. The maximum discrepancy on measurements repeated at 30 stations was of about ±0.05mGal. Our gravity reference datum is arbitrary, due to the absence of an absolute gravity bench- mark nearby the area under study, to which refeer our data to obtain absolute gravity anomalies.

Data reduction

The topographic relief within the study area (Figure 3) is very smooth, showing a slope trending eastward at about 20 m per km. The free-air gravity anomaly (Figure 4) was computed using the International Gravity Formula of 1967,

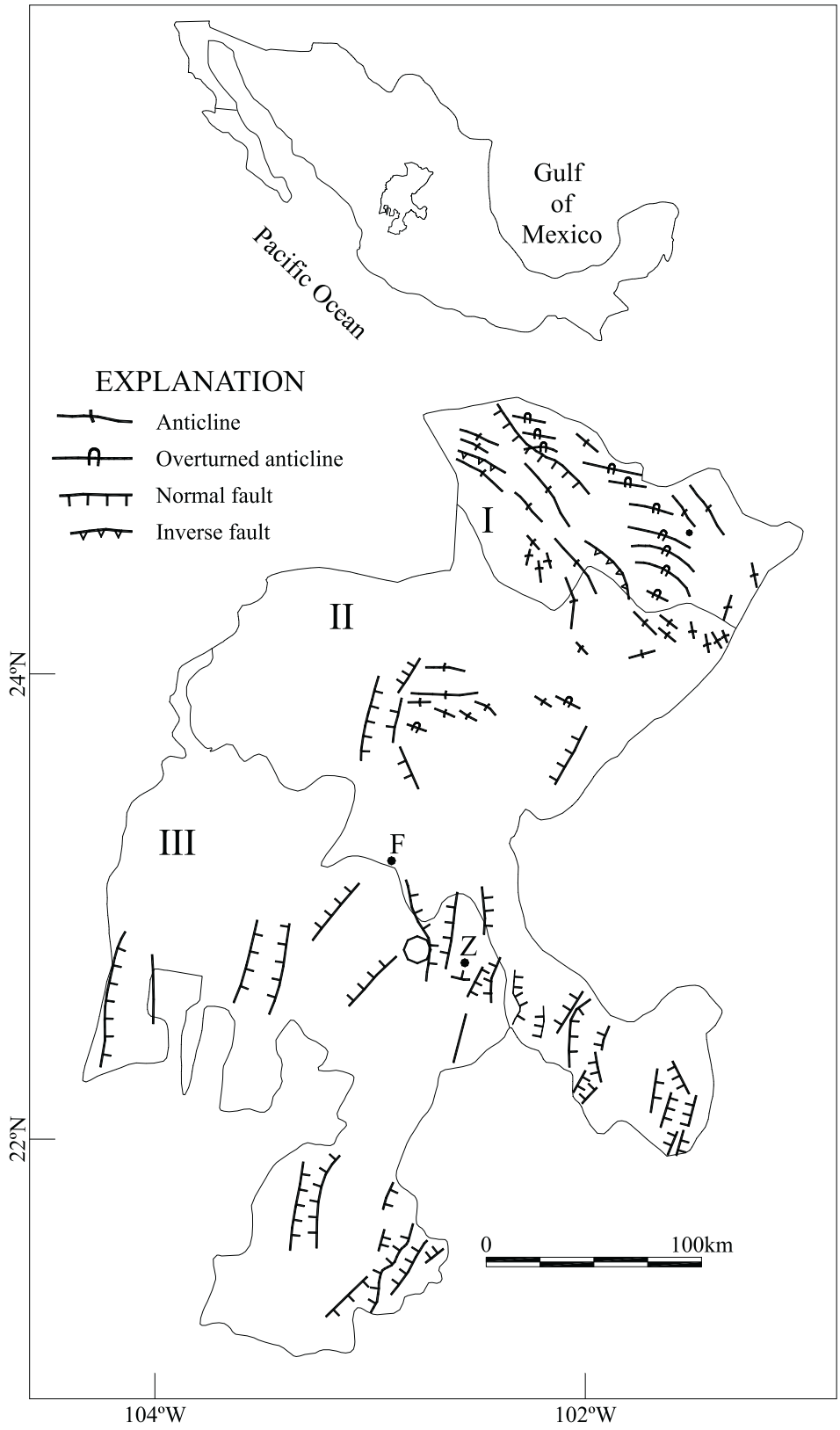

Fig. 1. Location map showing the Zacatecas State, regional geologic structures, and physiographic provinces: I Sierra Madre Oriental, II Mesa Central, and III Sierra Madre Occidental. F = Fresnillo City, Z = Zacatecas City. The study area is indicated with a circle. Adapted from CRM (1991).

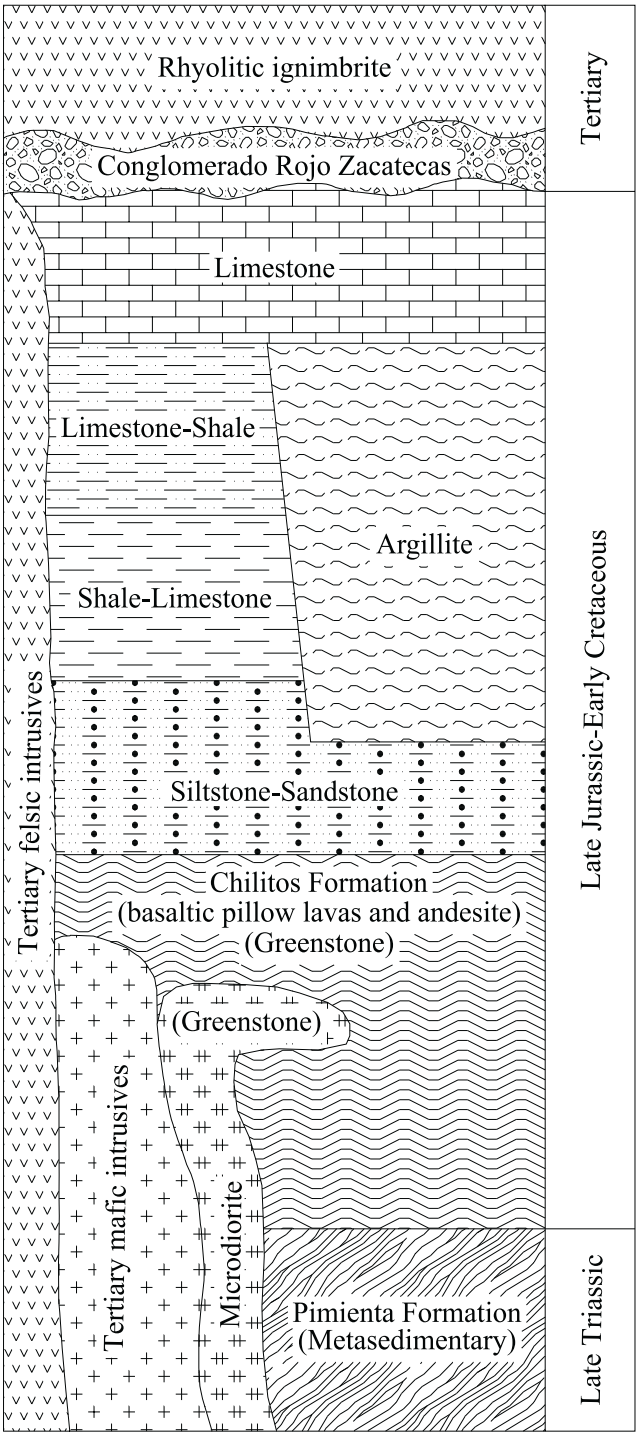

Fig. 2. Generalized stratigraphic column for the study area (adapted from CRM, 1991).

and the standard vertical gradient of 0.3086 mGal/m. To obtain a residual complete Bouguer anomaly, a terrain correction was carried out over a region that extends some 50 km beyond the study area. The terrain correction was computed using a digital model of elevation, with samples at every three seconds of arc, which corresponds to a length of about 90 m (INEGI, 1995). The elevations from the digital model, merged with the survey data, were gridded with nodes at every 50 m within the study area, and outside of the surveyed area with nodes at 100 m. The topographic relief was modeled by a collection of prisms. At the center of every grid node a prism with length and width equivalents to a grid cell was placed, and it extended down to sea level. The gravity effect at the i-th station, caused by a collection of *M* prisms is given by

$$g_i = \sum_{j=1}^{M} G_{ij}, \quad i = 1, N, \tag{1}$$

where

$$G_{ij} = \gamma\rho\left\{aLog(b+r) + bLog(a+r) - c\tan^{-1}\frac{ab}{cr}\right\} \begin{vmatrix} X_2 & Y_2 & Z_2 \\ X_1 & Y_1 & Z_1 \end{vmatrix}, \tag{2}$$

is the solution given in Banerjee and Gupta (1977) to compute the gravity effect caused by one prism of constant mass density, at the station of coordinates (x_i, y_i, z_i). In equation (2) γ is the Newtonian gravitational constant, ρ is the mass density of the prism, $a = x_j - x_i$, $b = y_j - y_i$, $c = z_j - z_i$, and $r = (a^2 + b^2 + c^2)^{1/2}$, where the variables ($x_j$, y_j, z_j, j=1,2) are coordinates of the prism vertex, and take values corresponding to the limits of integration shown in equation (2). The prism has length $l = Y_2 - Y_1$ and width $w = X_2 - X_1$, along the y and x directions, respectively, and it has a thickness $t = Z_2 - Z_1$, where Z_2 and Z_1 are depth to the top and bottom of the prism.

The gravity effect caused by this collection of *M* prisms was computed at the grid nodes of the the digital elevation model, within the study area, with a mass density of 2740 kg/m^3 corresponding to the limestone that hosts the ore body. This gravity effect (Figure 5) was then interpolated at the gravity stations using a bicubic spline algorithm (Press *et al*., 1986), and then subtracted from the free-air anomaly. The resulting terrain-corrected gravity anomaly (Figure 6) shows no correlation with topography, and strongly suggests a 3-D structure located north of the study area.

Regional-residual separation

The next step in the data reduction is the separation of the measured field into its regional and residual components. This separation is carried out by removing a smooth component that follows the broad features of the Bouguer gravity anomaly, which is attributed to regional geologic structures. However, the success of the separation relies on the interpreter's knowledge of the regional and local geology, along with an educated guess regarding the amplitude of local anomalies.

The regional component is assumed to corresponds to a polynomial surface, fitted to the data in the least-squares

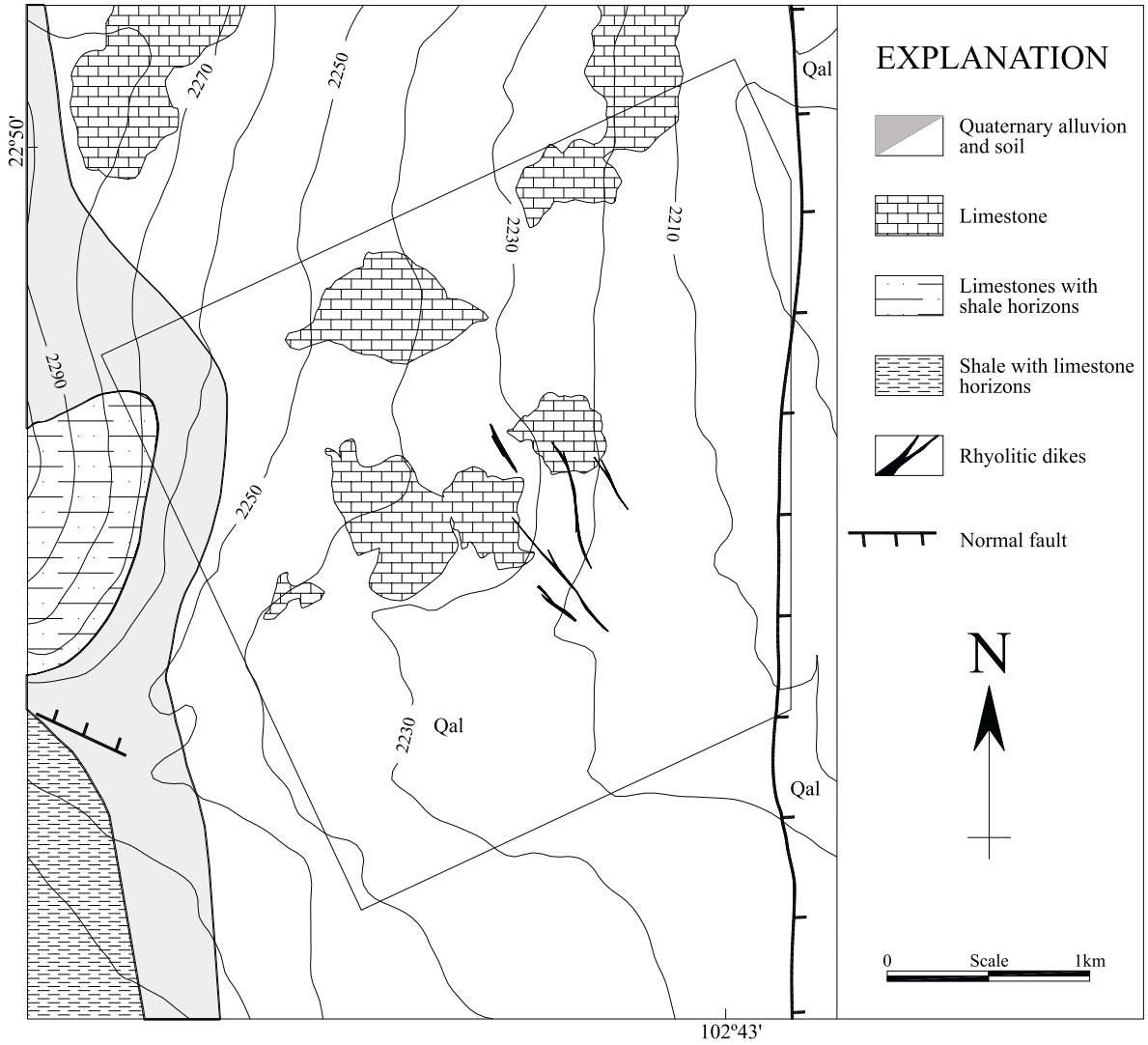

Fig. 3. Simplified geologic map of the study area adapted from CRM (1991). The gravity survey was conducted in the area enclosed by the polygon.

sense. After several trials, by just removing a first-degree polynomial surface, the resulting residual Bouguer anomaly was consistent with the known thickening of the top-soil and sediments surrounding the study area. The residual anomaly (Figure 7) shows a gravity high located at the northern part of the study area, surrounded by negative values.

Horizontal gravity gradient

The squared magnitude of the horizontal gravity gradient is given by

$$h(x,y) = |\nabla g(x,y)|^2 \qquad (3)$$

where

$$\nabla = \left(\frac{\partial}{\partial x}\mathbf{i} + \frac{\partial}{\partial y}\mathbf{j} \right). \qquad (4)$$

The partial derivatives of gravity with respect of the *x* and *y* directions were obtained in the wave number domain following methods described in Blakely (1995). The squared magnitude of the horizontal gradient of a gravity anomaly is a useful transformation, because it tends to place narrow ridges over edges of abrupt changes in density, providing a first order estimate of the source body horizontal dimensions. For the area under study (Figure 8) this transformation suggests that the ore body is constrained in an area of about 1.0 km^2.

THE NONLINEAR INVERSE PROCEDURE

The geometry of the model used in this interpretation consists of *M* contiguous, vertical, rectangular prisms of constant mass density. The location and the length and width of the prisms were kept constant. The free parameters of the

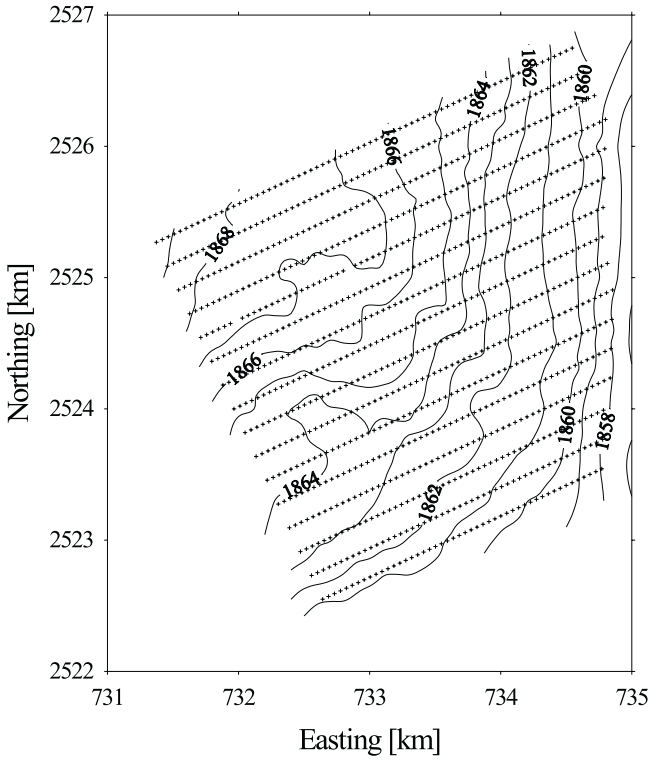

Fig. 4. Free-air gravity anomaly map of the study area, showing the location of gravity stations. The contour interval is one mGal. Coordinates correspond to a UTM projection for the Central Meridian 105°*W*.

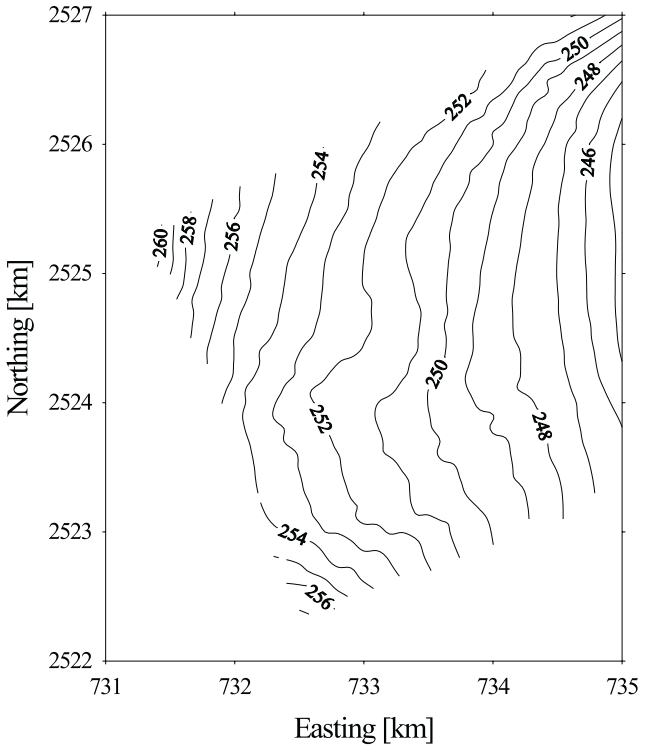

Fig. 5. Terrain corrections for the study area computed using a density of 2740 kg/m^3, the contour interval is one mGal.

model are either the depth to the top or bottom of the prisms. Let the *N* observed gravity data be represented by the vector $\mathbf{d} \in E^N$, and let the model response be the vector $\mathbf{g} \in E^N$. The forward model is a function of *M* parameters, which are elements of a vector $\mathbf{m} \in E^M$, representing either the depth to the top or bottom of the prisms. Using this notation, the solution of the forward problem given in equation (1) can be expressed as

$$\mathbf{g} = \mathbf{G}(\mathbf{m}) \, . \tag{5}$$

The vector **m** in equation (5) has a nonlinear relationship with **g**. Non-linear problems can be solved in successive approximations using the least squares method. This involves conversion of the non-linear problem into an approximated linear form by expanding to first order the functional **G**(**m**) in equation (5) in Taylor series about an initial trial $\mathbf{m}^0$ of what the model parameters might be:

$$\mathbf{G}(\mathbf{m}) \approx \mathbf{G}(\mathbf{m}^0) + \mathbf{J}\delta\mathbf{m}\delta \, , \tag{6}$$

where **J** is the *N*x*M* Jacobian matrix of partial derivatives of **G**(**m**) with respect of the model parameters evaluated at $\mathbf{m}^0$, with elements

$$J_{i,j} = \frac{\partial G_{i,j}}{\partial m_j} , \tag{7}$$

and vector $\delta\mathbf{m}=\mathbf{m}-\mathbf{m}^0$ is a perturbation in the parameters m_j. Using equation (6), the residual error vector $\mathbf{e}=\mathbf{d}-\mathbf{G}(\mathbf{m}^0)$, representing the difference between the model response for the trial vector $\mathbf{m}^0$ and the observed data, is found from

$$\mathbf{e} = \mathbf{J}\delta\mathbf{m} \, . \tag{8}$$

Following the Marquardt-Levenberg method (Levenberg, 1944; Marquardt, 1963), the perturbation in **m** is found minimizing an objective functional ϕ that is a function of the vectors $\mathbf{e} - \mathbf{J}\delta\mathbf{m}$ and $\delta\mathbf{m}$, subject to the constraint that $\delta\mathbf{m}^T\delta\mathbf{m} = \delta_0^2$ (Lines and Treitel, 1984):

$$\phi = (\mathbf{e} - \mathbf{J}\delta\mathbf{m})^T(\mathbf{e} - \mathbf{J}\delta\mathbf{m}) + \lambda(\delta\mathbf{m}^T\delta\mathbf{m} = \delta_0^2) \, , \tag{9}$$

where *T* means transpose and λ is known as the damping factor. Differentiation of equation (9) with respect of $\delta\mathbf{m}$, and setting to zero the result, yields the normal equations

$$\left[\lambda\mathbf{I} + \mathbf{J}^T\mathbf{J}\right]\delta\mathbf{m} = \mathbf{J}^T\left[\mathbf{d} - \mathbf{G}(\mathbf{m}^0)\right] \, . \tag{10}$$

The system of equations (10) is solved using LU decomposition, with forward elimination and back substitution. The Jacobian matrix **J** was obtained numerically following a finite difference numerical method (Atkinson, 1989). The present iterative procedure consists of solving the forward problem for an initial trial value for the solution

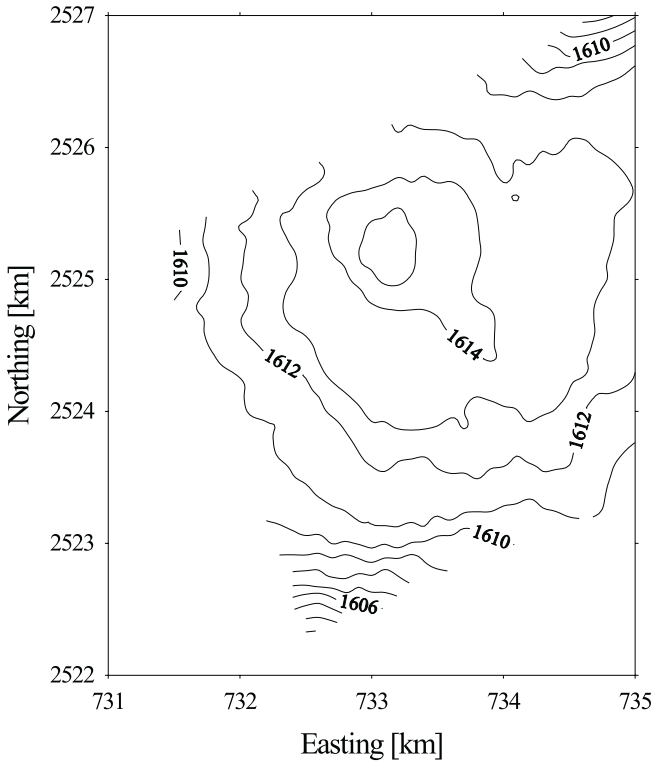

Fig. 6. Complete Bouguer gravity anomaly. The contour interval is one mGal.

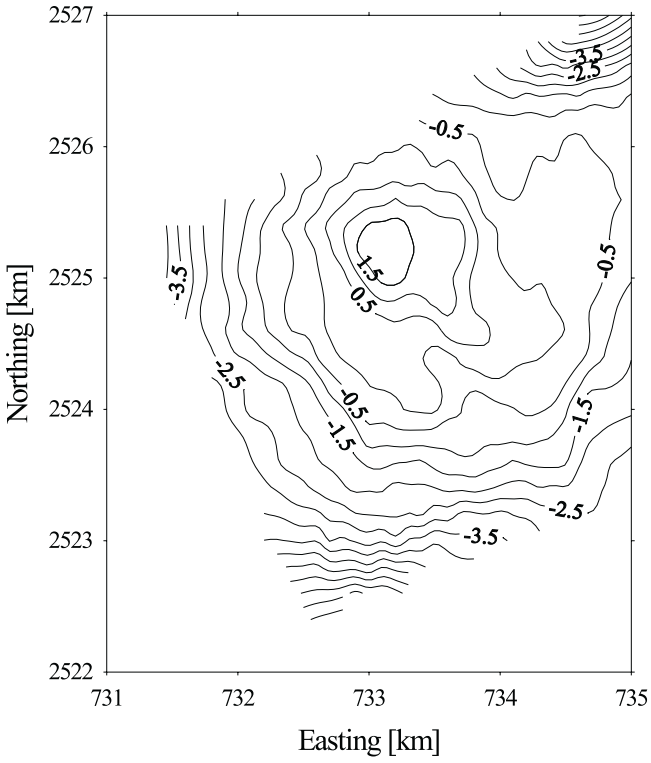

Fig. 7. Residual Bouguer gravity anomaly. The contour interval is one half of mGal.

vector $\mathbf{m}^0$, along with the size of the residual error vector $\boldsymbol{q}^0=\mathbf{e}^T\mathbf{e}$. Next, the Jacobian matrix is computed, the system of equations (9) is solved with an initial damping factor λ=1, and a new solution is computed using the vector $\mathbf{m}^1=\mathbf{m}^0+\delta\mathbf{m}$. If in the new solution $q^1<q^0$, the damping parameter is reduced to one half of its initial value, and a new solution $\mathbf{m}^2$ is found. This iterative process continues until an acceptable solution is reached, or when no further improvement in the solution is achieved. At the last iteration the root-mean-squared (rms) misfit error, given by

$$rms = 100 \times \sqrt{\sum_{i=1}^{N} (d_i - g_i^k)^2} \Big/ \sqrt{\sum_{i=1}^{N} d_i^2}\,, \qquad (11)$$

is computed, where g_i^k is the forward model solution at the k-th iteration.

Constrains and assumptions

From a hole drilled near the center of the gravity high (Figure 6) is known the following independent information: The top of the ore body was reached after drilling 50 m, at about 2185 m asl. It had a thickness of some 85 m, and is mainly sphalerite with an average density of 3200 kg/m^3. The ore body is hosted in limestone with an average density of 2740 kg/m^3. Consolidated sediments with an average density of 2240 kg/m^3 overly the limestone unit.

If we consider the area of the circular region inferred from the gravity gradient analysis (Figure 8), the thickness of the ore body determined by the drill-hole, and its average density, upper bounds for the volume and the mass of the ore body are of about $85\times10^6 m^3$ and 272×10^6 metric tons, respectively.

To carry out the inversion of gravity data, a simple model which consists of three lithologic units with constant mass density contrast is assumed. The first is a sedimentary unit with a density contrast of -500 kg/m^3, the second corresponds to the limestone unit with zero density contrast, and a third unit represents the ore body with a density contrast of 460 kg/m^3.

Application of the method

The gravity and topographic data were gridded, using a minimum curvature algorithm, with nodes at 200 m in the north-south direction, and nodes at 100 m in the east-west direction (Figure 9-a). The approach in modeling the residual Bouguer gravity data uses the principle of superposition of potential fields (Blakely, 1995). Thus the gridded gravity data

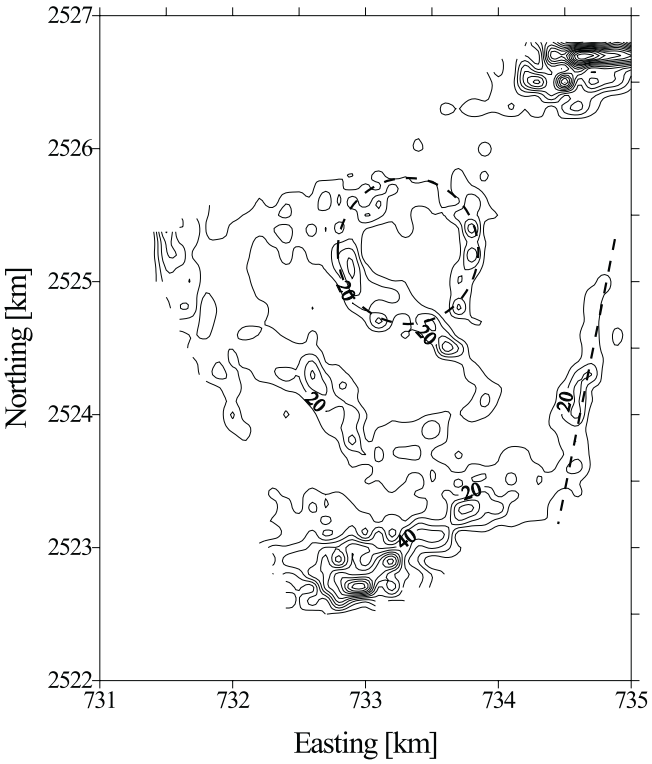

Fig. 8. The magnitude of the horizontal gravity gradient for the study area is shown with contours every 20 [mGal/km]^2. The dashed line suggests the presence of a fault. The lateral extension of the source body (~1.0 km^2) and its location are indicated by the circle.

were then divided into two data sets of 122 positive and 476 negative values respectively. To keep an evenly determined algebraic problem, a prism is associated with every gravity data, and each data subset is modeled independently. Physically, this approach implies that the sedimentary unit and ore body are uncoupled, and completely separated by the presence of the limestone unit.

In order to account for the negative subset of residual gravity data, the upper part of the prisms was made to coincide with the topography. In the first trial every prism has a thickness $t = 0$, and a density contrast $\Delta\rho = -500$ kg/m^3. Thus, the base of all of the prisms is allowed to move downwards, until it fits the negative part of the residual Bouguer gravity anomaly. After 15 iterations, a *rms* misfit error of about 0.7% was obtained. It is worth to point out here that because of the limited horizontal extension of the model, the thickness of prisms located at the edges of the study area tends to be excessive. The estimated interface between the sedimentary unit and the limestone unit is shown in Figure 9-b.

To account for the positive subset of residual gravity data, the 1-2 m thick superficial residual soil that covers the limestone unit was neglected. According to drill hole data, the ore body ends at 2100 m asl; thus the bottom of all of the prisms was kept constant at such depth. For all of the prisms the density contrast was $\Delta\rho = 460$ kg/m^3. Initially, to avoid any bias from the initial trial, a thickness $t = 0$ was assigned to all the prisms. Thus the thickness are automatically increased, by moving upwards the top of the prisms, until no further improvement is obtained. At the end of this process, after 15 iterations, a *rms* misfit error of about 3.6 % was obtained. Shown in Figure 9-c is the upper surface of the interpreted ore body.

The superposition of the gravity effects caused by the modeled ore body and the sedimentary unit is shown in Figure 9-d, and this is compared with the observed residual gravity anomaly. Thus, the validity of the separation between negative an positive gravity values can be judged in base of the fair fit obtained between the observed and computed gravity anomalies.

An economic volume of about 70×10^6 m^3 is found by adding the volume of all prisms used to model the ore body. The estimated mass is of about 150×10^6 metric tons assuming a mass density of 3200 kg/m^3.

CONCLUSIONS

A simple approach for non-linear, constrained, 3-D inversion of gravity data, based on the principle of superposition of potential fields is demonstrated. The method assumes that all data are pure signal and attempts to match all observations equally. The vertical extension of the ore body and densities, determined from one drillhole, were used to constrain the solution. The magnitude of the horizontal gravity gradient provided an additional estimate for the location and lateral extension of the ore body. Edge effects are caused by the finite source volume and the limited extent of the data region. Thus, it is likely that, at the edges of the study area, the thickness of the sedimentary unit has been overestimated. The application of this method on the complete residual Bouguer gravity anomaly allowed to estimate a 3-D geometry of the ore body. From this interpretation an economic volume of about 70×10^6 m^3 and a mass of about 150×10^6 metric tons are estimated. The procedure presented here may provide an initial estimate of the shape of the ore body, to target an exploratory drilling program.

ACKNOWLEDGMENTS

The author gratefully acknowledged the comments on previous versions of the manuscript by Carlos F. Flores-Luna, Luis Delgado-Argote, Francisco J. Esparza-Hernández, and Lance Forsythe. Victor M. Frias-Camacho is also acknowledged for its help in drafting the figures. The critical and yet constructive review by Oscar Campos-Enríquez, one anonymous reviewer, and by Cinna Lomnitz, helped me to improve the contents.

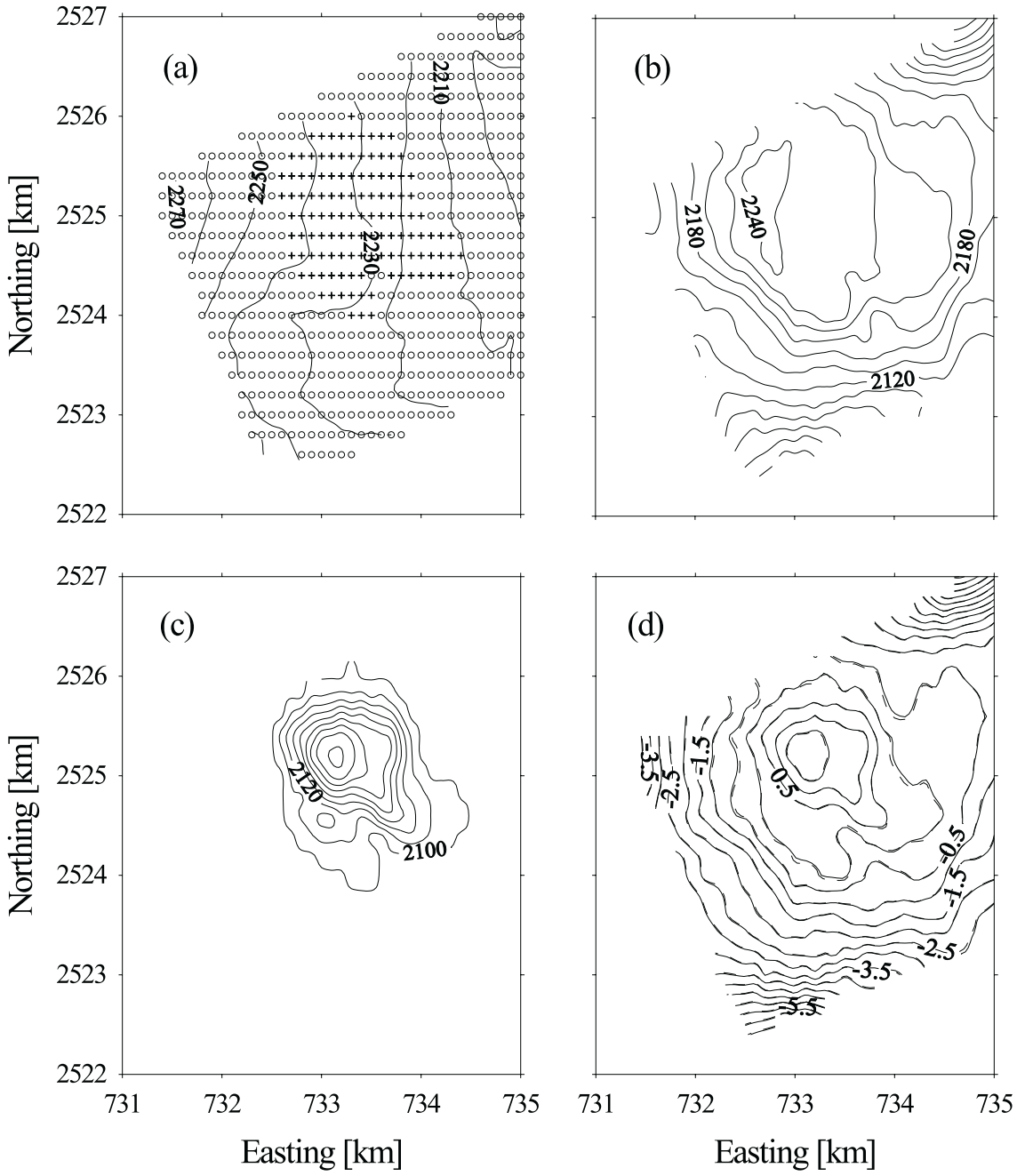

Fig. 9. (a) The topography used to constrain the model is shown with contours at every 10 m. The open circles (negative values) and the plus (positive values) symbols indicate the locus of the prisms used to model the sedimentary unit, and the ore body, respectively. (b) Shown with contours at every 20 m is the base of the prisms that represent the interface between the sedimentary and the limestone unit that hosts the ore body. (c) Shown with contours every 10 m are the top of the prisms that represent the interface between the ore body and the limestone unit. (d) The observed residual Bouguer gravity anomaly (solid line), with contours every 0.5 mGal, is compared with the gravity effect caused by the model obtained from the inversion (dashed line).

BIBLIOGRAPHY

ATKINSON, K. E., 1989. An introduction to numerical analysis. John Wiley & Sons, Inc., 693 pp.

BANERJEE, B. and S. P. D. GUPTA, 1977. Gravitational attraction of a rectangular parallelepiped. *Geophys., 42*, 1053-1055.

BLAKELY, R. J., 1995, Potential theory in gravity and magnetic applications. Cambridge University Press, 441 pp.

CORDELL, L. and R. G. HENDERSON, 1968. Iterative three-dimensional solution of gravity anomaly data using a digital computer. *Geophys., 33*, 596-601.

CRM (Consejo de Recursos Minerales), 1991. Monografía Geológico Minera del Estado de Zacatecas. Publicación M-2e, Pachuca, Hidalgo, México, 154 pp.

CHAI, Y. and W. J. HINZE, 1988. Gravity inversion of an interface above which the density contrast varies exponentially with depth. *Geophys.*, *53*, 837-845.

GARCIA-ABDESLEM, J., 1996. Comments on "Gravity field of the southern Colima graben". *Geofís. Int*., *35*, 87-88.

GARCIA-ABDESLEM, J, 1995. Inversion of the power spectrum from gravity anomalies of prismatic bodies. *Geophys.*, *60*, 1698-1703.

GARCIA-ABDESLEM, J, 1992. Gravitational attraction of a rectangular prism with depth dependent density. *Geophys.*, *57*, 470-473.

BEAR, G. W., H. J. AL-SHUKRI and A. J. RUDMAN, 1995. Linear inversion of gravity data for 3-D density distributions. *Geophys.*, *60*, 1354-1364.

HENRY, C. D. and J. J. ARANDA-GOMEZ, 1992. The real southern Basin and Range: Mid- to late Cenozoic extension in Mexico. *Geology*, *20*, 701-704.

INEGI (Instituto Nacional de Estadística, Geografía e Informática), 1995. Modelo digital del elevaciones de la República Mexicana en disco compacto Aguascalientes, Aguascalientes, México.

LEVENBERG, K., 1944. A method for the solution of certain nonlinear problems in least squares. *Quart. Appl. Math*., *2*, 164-168.

LINES, L. R. and S. TREITEL, 1984. A review of least-squares inversion and its application to geophysical problems. *Geophys. Prosp.*, *32*, 159-186.

MADEIROS, W. E. and J. B. C. SILVA, 1995. Gravity source moment inversion: A versatile approach to characterize position and 3-D orientation of anomalous bodies. *Geophys.*, *60*, 1342-1353.

MARQUARDT, D. W., 1963. An algorithm for least squares estimation of nonlinear parameters. *J. SIAM, 11*, 431-441.

PONCE, B. F. and K. F. CLARK, 1982. The Zacatecas mining district: A Tertiary caldera complex associated with precious and base metal mineralization. *Economic Geology*, *83*, 1668-1682.

PRESS, W. H., B. P. FLANNERY, S. A. TEUKOLSKY and W. T. VETTERLING, 1986. Numerical Recipes, Cambridge Univ. Press, 963 pp.

SALAS, G. P., 1975. Carta y provincias metalogenéticas de la república Mexicana. Consejo de Recursos Minerales, México, D.F., Pub. 21E, 242 pp.

VAIL, P. R., R. M. Jr. MITCHUM and S. THOMPSON, III, 1977. Global cycles of relative changes of sea level. *In:* Seismic Stratigraphy - Applications to Hydrocarbon Exploration, ed. C. E. Payton. *AAPG*, Memoir 26, pp. 83-97.

ZEYEN, H. and J. POUS, 1993. 3-D joint inversion of magnetic and gravimetric data with *a priori* information. *Geophys. J. Int*., *112*, 244-256.

———

J. García-Abdeslem[1]
[1] *CICESE, División de Ciencias de la Tierra, Departamento de Geofísica Aplicada, km 107, Carretera Tijuana-Ensenada, Ensenada, B. C., México 22830.*